Advances in Fabry-Perot and Tunable Quantum Cascade Lasers

C. Kumar N. Patel

Pranalytica, Inc., 1101 Colorado Avenue, Santa Monica, CA 90401

INTRODUCTION

Quantum cascade lasers (QCLs) are becoming mature infrared emitting devices that convert electrical power directly into optical power and generate laser radiation in the mid wave infrared (MWIR) and long wave infrared (LWIR) regions. These lasers operate at room temperature in the 3.5 μm to >12.0 μm region. QCLs operate at longer wavelengths into the terahertz region; however, these require some level of cryogenic cooling. Nonetheless, QCLs are the only solid-state sources that convert electrical power into optical power directly in these spectral regions.

Three critical advances have contributed to the broad range of applications of QCLs, since their first demonstration in 1994 [1]. The first of these was the utilization of two phonon resonance for deexcitation of electrons from the lower lasing level [2]; the second is the utilization of epi-down mounting with hard solder of QCLs for practical applications [3]; and the third is the invention of non-resonant extraction for deexciting electrons from the lower laser level and simultaneously removing constraints on QCL structure design for extending high power room temperature operation to a broad range of wavelengths [4].

Although QCLs generate CW radiation at room temperature at wavelengths ranging from ~3.5 μm to >12.0 μm, two spectral regions are very important for a broad range of applications. These are the first and the second atmospheric transmission windows from ~3.5 μm to ~ 5.0 μm and from ~8.0 μm to ~12.0 μm, respectively. Both of these windows (except for the spectral region near 4.2 μm, which is dominated by the infrared absorption from atmospheric carbon dioxide) are relatively free from atmospheric absorption and have a range of applications that involve long distance propagation.

FABRY-PEROT (FIXED WAVELEGNTH BROAD BAND) OPERATION

Table 1 provides a concise summary of the QCL performance that has been reported for room temperature CW operation requiring thermoelectric coolers (TEC) for thermal management and quasi-continuous wave (QCW) operation (high duty cycle pulsed) not requiring TECs, thus making QCW operation for battery operated, hand held laser system operation. The Table shows data for CW and average power outputs from QCLs fully packaged in hermetically sealed butterfly packages together with beam collimating optics and TECs for CW operation [5-8]. It should also be pointed out that CW power output of ~5.0 W

has been reported from QCLs in probably not fully packaged versions at wavelengths somewhat longer than 5.0 μm [9].

Table 1. Summary of Power Output Performance of CW and QCW Quantum Cascade Lasers

FP Center Wavelength	CW/RT Power (FP Geometry, Requires TEC)	QCW/RT Average Power (FP Geometry, No TEC)
3.8 μm	> 1.5 W	>1.0 W
4.0 μm	> 2.5 W	>2.0 W
4.6 μm	> 4.0 W	>3.0 W
5.3 μm	> 1 W	>1.0 W
6.2 μm	>1 W	>1.0 W
6.8 μm	~ 1 W	>1.0 W
7.2 μm	~ 1.4 W	>1.5 W
8.2 μm	~ 1 W	>1.5 W
9.2 μm	~ 2.0 W	>2.0 W
10.2 μm	~ 1 W	>1.0 W
10.6 μm	~ 500 mW	>500 mW
11.3 μm	~ 200 mW	>200 mW

The data presented above are representative of QCLs that configured to operate as Fabry-Perot devices with high reflectivity coating on the back facet and controlled reflectivity coating on the front facet. Output form such lasers occurs in a broad linewidth, ~150 nm to 300 nm wide, around the design center wavelength of the QCL.

In addition to the power output, one more performance parameter is important for technological applications of QCLs. This is the wall plug efficiency (WPE), which is the efficiency with which the QCL converts electrical power into optical power. Table 2 provides a summary of WPE achieved for practical, fully packaged QCLs. Two recent advances point to potential breakthroughs here. The first is the two material active region design [10], which has shown WPE of ~28% at a wavelength of ~5.6 μm and a reduced number of gain stages design [11, 12].

Table 2. Summary of WPE of CW and QCW Quantum Cascade Lasers

FP Center Wavelength	CW/RT WPE (FP Geometry, TEC Power Not Included)	QCW/RT WPE (FP Geometry, Over All Efficiency, Including the Pulse Driver)
3.8 µm	~5 %	~5 %
4.0 µm	~10 %	~7 %
4.6 µm	~16 %	>10 %
7.2 µm	~10 %	~12 %
9.2 µm	~10 %	~10%

The good WPE achieved to date in practical, fully packaged devices has made it possible significant miniaturization of fully packaged QCLs for practical applications. Figure 1 shows the smallest footprint QCW operation quantum cascade laser, to date, that weighs less than 50 g (2 Oz) including the electronics driver and produces >3.5 W of average power at a wavelength of ~4.6 µm. The laser system requires only 12VDC-20VDC electrical input. Figure 2 shows a fully packaged, tabletop system that includes the laser package shown in Figure 1 and rechargeable batteries. The total weight, including batteries, is less than 450 g (<16 Oz).
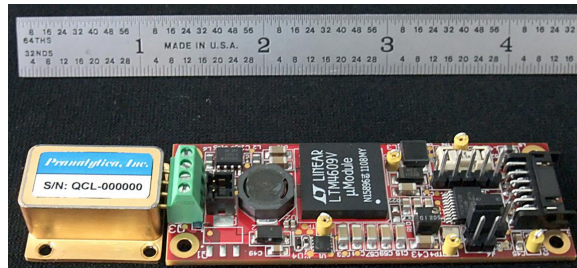

Figure 1. Miniaturized packaged QCW operation QCL. Total weight is <50 g (<2 Oz) and the laser produces an average power of >3.5 W at a wavelength of ~4.6 µm.

Figure 2. Packaged QCW operation QCL of Figure 1, including rechargeable batteries, weighs less than 450 g (<16 Oz) and produces >3.5 W of average power at a wavelength of ~4.6 µm.

FP configuration, broad band output QCLs are ideally suited for high power applications, including laser sources for directed infrared countermeasures for protecting aircraft from shoulder fired missiles (MANPADS), infrared target pointer, illuminators and designators and infrared IFF beacons. These applications are expanding very rapidly.

NARROW LINEWIDTH (EXTERNAL GRATING CAVITY) OPERATION

As mentioned earlier, Fabry-Perot configuration QCL generate significant amount of infrared power in very broad bandwidth, reflecting the width of gain spectrum of the QCL. For many applications, however, one needs narrow linewidth output that either is fixed in wavelength at a preset value or is variable under user's control. These applications include laser power interaction with materials that is dependent on the laser wavelength. These general class of applications include laboratory and research spectroscopic investigation, detection of pollutants, detection of chemical warfare agent, explosives and toxic industrial chemical, environmental monitoring, in-line real-time process monitoring in semiconductor fab lines, product quality assurance in health care industries, real-time process monitoring in bio-pharma industries, monitoring spoilage in food, vegetable and fruit storage facilities and fermentation monitoring in wine production.

A widely used technique for converting broadband output from a Fabry-Perot configuration laser into narrow bandwidth output is to replace one of the reflecting surfaces of laser with a wavelength dispersive device such as a grating or a prism. Typically a macroscopic grating is used as schematically shown in Figure 3. This scheme has been successfully used with all types of broad band optical gain sources, including dye lasers, optically pumped solid state lasers and near IR junction semiconductor lasers. Over the past ten years, the external grating cavity tunable geometry has been extensively used with quantum cascade lasers, which permit a coverage from ~3.5 µm to >12.0 µm using QCLs with multiple center wavelengths.
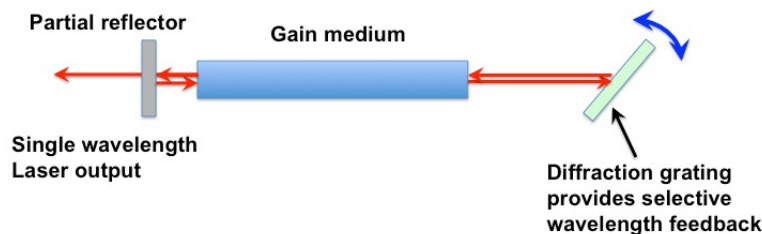

Figure 3. Typical external grating cavity configuration for extracting narrow band tunable power output from a broadband gain source (Littrow geometry)

Almost all of today's tunable quantum cascade lasers utilize the configuration shown in Figure 3 or its slight variant, the Littman geometry. Successful as these laser tuning techniques are, they suffer from two serious deficiencies:

1. Susceptibility to shock and vibration: For many real life applications, especially those where the tunable laser source is mounted on a moving platform, such a vehicle or manned (airplanes, helicopters, etc.) or unmanned aircraft (UAVs), immunity for shock and vibration, both during non-operation times as well as during operations is very important. A good example of this requirement is a tunable laser mounted on a Humvee traveling at 30 mph for standoff identification of IEDs at safe distances without stopping the vehicle. The traditional tunable QCL configuration (Figure 3) does not meet he requirements because the macroscopic diffraction grating needs to be physically rotated around its axis for laser wavelength tuning and ruggedizing this mechanism such that it operates reliably when vibration/shocks are present is a daunting task.

2. Tuning speed: The speed of tuning of conventional grating tuned lasers (Figure 3) is slow because of the mechanical rotation of the diffraction grating. Fastest tuning speed reported is 10 ms for a scan from one edge of the tunable spectrum to the other covering ~200 cm^{-1}, which yield a tuning speed of ~2 x 10^4 cm^{-1} sec^{-1}. Moreover, for random switching between wavelengths, speed could even be slower. One can achieve somewhat faster speeds, about a factor of five faster, by either including an intracavity vibrating mirror or MOEMs mounted gratings. However, for either of these cases, the wavelength scan is limited. What is needed is a tuning speed of <1 µs for either random switching of wavelengths or < 20 µs for scanning across the entire tuning spectral range of the QCL (> 200 cm^{-1}). Thus, required tuning speeds are >2 x 10^8 cm^{-1} s^{-1}, i.e., four orders of magnitude faster than that's possible with the conventional wavelength scanning mechanism.

The limitations, above, point to the need for a new wavelength tuning mechanism that does not rely on mechanical rotation of a diffraction grating. We have explored electronic tuning to accomplish what is needed.

ALL ELECTRONIC TUNING OF QUANTUM CASCADE LASERS

We have used an acousto-optic modulator (AOM) for creating an electronically controlled grating for tuning of infrared quantum cascade lasers [13]. AOM tuning of dye lasers and semiconductor lasers in the visible and near infrared spectral regions has been demonstrated earlier [14, 15]. Figure 4 shows a schematic of the AOM tuned QCL system.
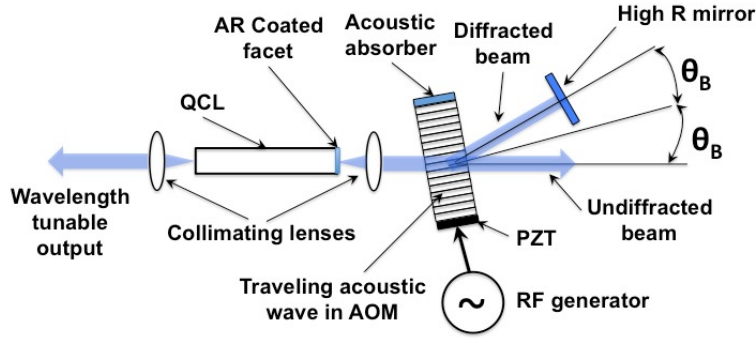
Figure 4. Acousto-optic (all electronic) tuning of quantum cascade lasers

The AOM tuned QCL has no mechanically moving parts for wavelength scanning. The RF signal injected into the acousto-optic modulator sets up pressure waves in the AOM crystal (Ge in the present case) at the RF frequency. Since there is an acoustic absorber at the other end of AOM crystal, the lack of acoustic reflection leads to the traveling pressure waves and corresponding spatial periodic variation in refractive index of the crystal, i.e., a traveling phase grating with grating spacing determined by the acoustic wavelength in the AOM crystal. The infrared radiation traversing the AMO crystal is therefore diffracted by the acoustic grating at the Bragg angle, θ_B, given by:

$$\sin\theta_B = \frac{m\lambda_0}{n\Lambda}$$ (1)

where, λ_0 is the optical wavelength,   is the optical refractive index of the AOM crystal, and Λ is the acoustic wavelength. Placing a reflector as shown in Figure 4, the radiation at a wavelength determined by Eq. (1), is reflected back into the gain medium resulting in the laser producing radiation at the selected frequency. For a fixed placement of the back reflecting mirror as shown in Figure 4, changing the RF frequency will change the phase grating spacing in the AOM crystal and lead to a tuning of the wavelength of the radiation generated by the setup. Equation (1) can be manipulated to show that

$$f_0 = \frac{c}{nv_a\sin\theta}f_a$$ (2)

where, c is the velocity of light, v_a is the acoustic velocity in the AOM crystal and f_a is the acoustic (RF) frequency. We see that a given fixed angle for the setting of the back reflecting mirror, the optical wavelength varies linearly with the acoustic (RF) drive frequency.

Studies to date have concentrated on tunable QCLs in the 8 μm to 10 μm range because we have a broad gain structure QCL material and the AOM used is off-

the-shelf modulator designed for switching CO_2 lasers in the 9.6 μm and 10.6 μm regions. Present tunability on the 9 μm centered AOM tuned QCL system are shown in Figures 5 and 6, for QCW [13] and CW [16] operation of the lasers.
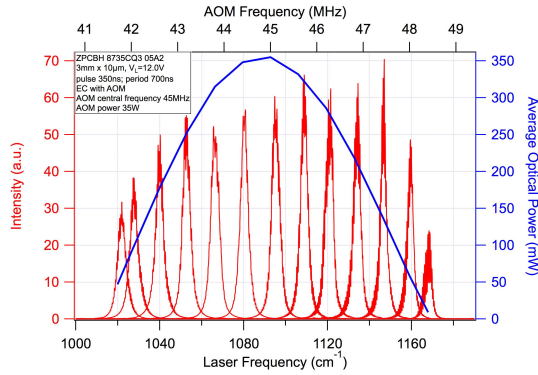

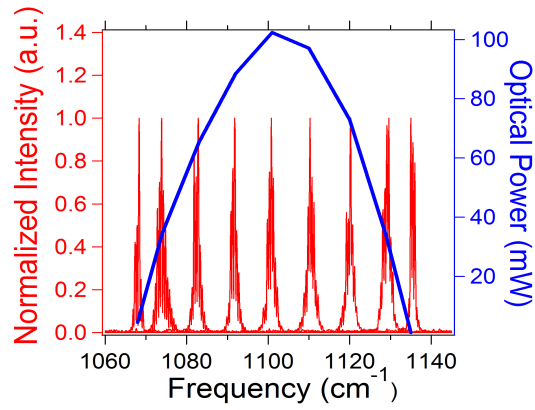**Figure 5. QCW operation tuning characteristics of AOM tuned QCL**

Figure 6. CW operation tuning characteristics of AOM tuned QCL

Measured linewidths vary from ~4 cm^{-1} for QCW operation [13] to ~1.5 cm^{-1} for CW operation [16].

Wavelengths are changed by changing the RF frequency. Wavelength switching time is measured by investigating the time it takes for the wavelength to change when following a change in RF frequency. The switching time, τ_{sw} is given by:

$$\tau_{sw} = \frac{\pi D_B}{v_a} \tag{3}$$

where, D_B is the diameter of the optical beam traversing the AOM. For our demonstration of AOM tuned QCL, $D_B = 2\,mm$ and $v_a = 5\cdot10^5\,cm\,s^{-1}$, we obtain $\tau_{sw} \approx 1\mu s$.

Figure 7 shows measurements of wavelength switching time. Top figure shows the geometry of the AOM switched QCL beam traversing the AOM. PZT at the left edge of the AOM crystal launches the acoustic wave, which traverses the laser beam position as shown. Initially (at t < 0), the RF frequency is set at 35 MHz, which as seen from Figure 5, is outside the range of spectral coverage provided by the QCL gain chip and no laser output is seen. At t=0, the RF frequency is changed to 45 MHz, which is at the peak of the laser output (Figure 5) at 1085 cm^{-1}. There is a latency period before laser output starts building up, corresponding to the acoustic pressure waves reach the position of the laser beam. At this time (t ~1.3 μs), the laser output starts building up and reaches a

steady state in ~550 ns, which is the switching time for laser wavelength. The latency time can be arbitrarily reduced by decreasing the physical distance of the laser position in the AOM crystal to zero by moving it closer to the PZT which launches the acoustic wave.
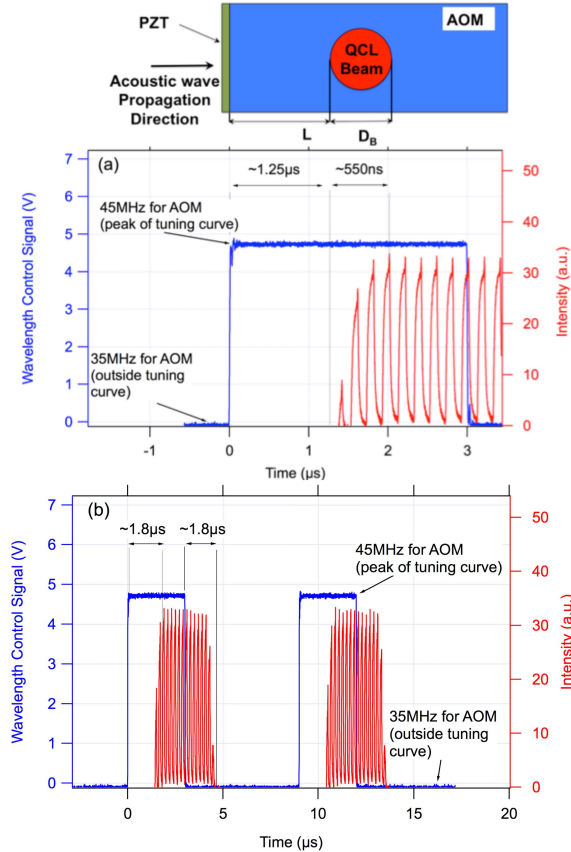

Figure 7. Switching time measurements of AOM tuned QCL

Two Wavelength Operation of AOM Tuned QCL

The response of the AOM crystal and the PZT are both linear and therefore, if instead of one RF frequency we were to launch two (or more) different RF frequencies, we would set up two independent phase gratings with different acoustic wavelengths. As seen from Eq. (2), this should result in simultaneous lasing at two wavelengths.

Figure 8 shows the schematic of the experimental setup for the demonstration of simultaneous two wavelength operation of the AOM tuned QCL. We are able to apply either one of the two RF frequencies independently or simultaneously [17]. Two wavelength operation in AOM tuned near infrared junction semiconductor lasers operating on two wavelengths has been reported earlier [18].
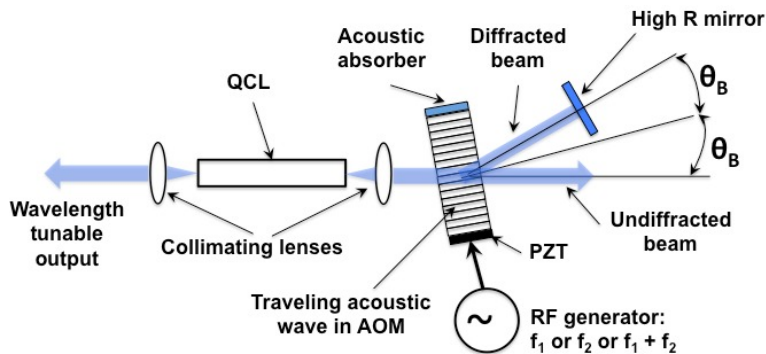
Figure 8. AOM tuned QCL setup for simultaneous two wavelength operation.

Figures 9 and 10 show laser output at 1088 cm^{-1} and 1118 cm^{-1} when RF frequencies of 30.5 MHz and 32.9 MHz are individually applied, respectively.
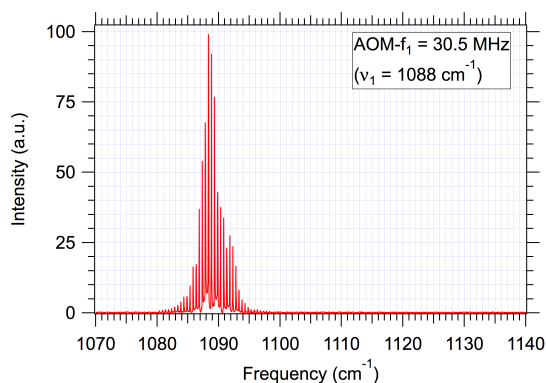

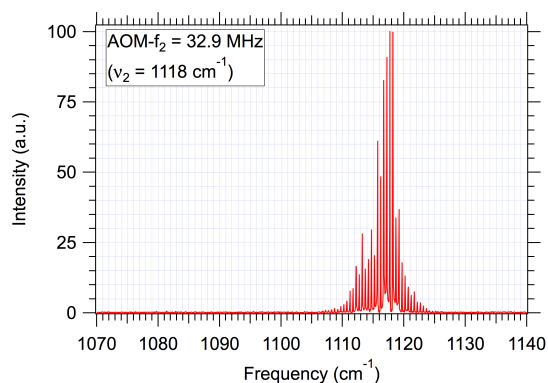**Figure 9. Laser output at 1088 cm^{-1} when RF frequency of 30.5 MHz is applied.**

Figure 10. Laser output at 1118 cm^{-1} when RF frequency of 32.9 MHz is applied.

Figure 11 shows the laser output when both the RF frequencies, 30.5 MHz and 32.9 MHz, are simultaneously applied. We see the simultaneous operation at two wavelengths has been achieved.
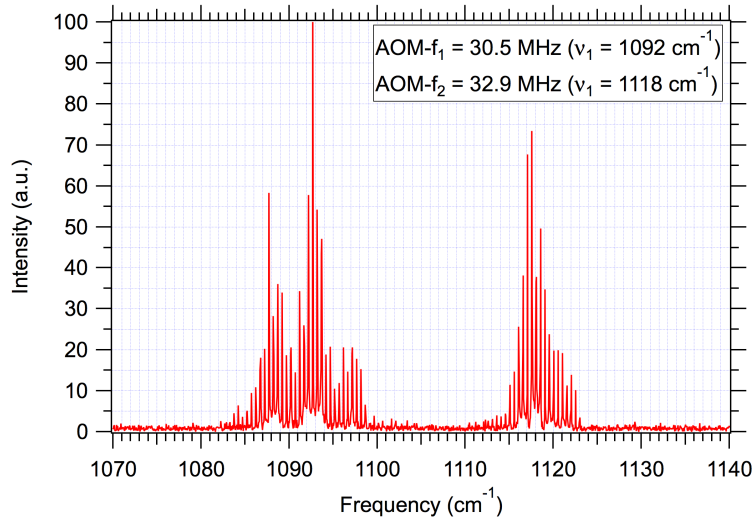
Figure 11. Simultaneous two wavelength operation of AOM tuned QCL

One of the important question to raise is how close can we bring the two simultaneously lasing wavelengths. As we have shown [17], hole burning in the gain spectrum of QCL determines how close we can bring the two wavelengths together. The natural linewidth (i.e., relaxation time) of the QCL levels responsible for the gain will be the determining factor as seen from Figure 12.
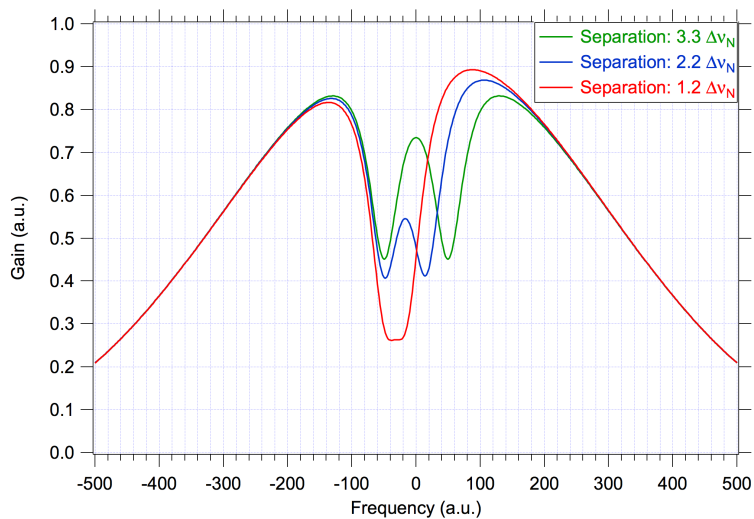

Figure 12. Hole burning schematic determining the smallest separation between two simultaneously lasing wavelengths.

From the experimentally determined smallest separation was 13 ± 5 cm^{-1}. This is a good approximation to the natural linewidth and yields a level relaxation time of 0.6 ps $\pm$ 0.2 ps. This is consistent with calculated lifetimes of 0.2 ps to 1.5 ps. It should be pointed that this experimental determination is an important because it reflects the level lifetimes in an actual high power operation of the QCL.

REFERENCES

[1] J. Faist, F. Capasso, D. L. Sivco, C. Sartori, A. L. Hutchinson and A. Cho, "Quantum Cascade Laser", *Science* **264,** 553-556 (1994).

[2] M. Beck, D. Hofstetter, T. Aellen, J. Faist, U. Oesterle, M. Ilegems, E. Gini and H. Melchior, "Continuous Wave Operation of a Mid-Infrared Semiconductor Laser at Room Temperature" *Science* **295**, 301 (2002).

[3] Alexei Tsekoun, Rowel Go, Michael Pushkasrsky, Manijeh Razeghi and C. Kumar N. Patel, "Improved Performance Of Quantum Cascade Lasers Via A Scalable, Manufacturable Epitaxial Side Down Mounting Process Utilizing Aluminum Nitride Heatsinks" *Proc. Nat. Acad. Sciences* **103,** 4831–4835 (2006).

[4] Arkadiy Lyakh, C. Pflügl, L. Diehl, Q. J. Wang, Federico Capasso, X. J. Wang, J. Y. Fan, T. Tanbun-Ek, R. Maulini, A. Tsekoun, R. Go and C. Kumar N. Patel, *Applied Physics Letters* 92, 111110 (2008).

[5] Arkadiy Lyakh, Richard Maulini, Alexei Tsekoun, Rowel Go and C. Kumar N. Patel, "Tapered 4.7 µm Quantum Cascade Lasers with Highly Strained Active Region Composition Delivering Over 4.5 Watts of Continuous Wave Optical Power", *Optics Express* **20 (4)** 4382-4387 (2012).

[6] A. Lyakh, R. Maulini, A. Tsekoun, R. Go, S. Von der Porten, C. Pflügl, L. Diehl, Federico Capasso and C. Kumar N. Patel, "High Performance Continuous-Wave Room Temperature 4.0 µm Quantum Cascade Lasers with Single-Facet Optical Emission Exceeding 2 Watts", *Proceedings of the National Academy of Sciences* **107,** 18799-18802 (2010).

[7] Richard Maulini, Arkadiy Lyakh Alexei Tsekoun and, C. Kumar N. Patel, "λ~7.1 µm Quantum Cascade Lasers with 19% Wall-Plug Efficiency at Room Temperature", *Optics Express,* **19,** 17203-17211 (2011).

[8] Arkadiy Lyakh, Richard Maulini, Alexei G. Tsekoun, Rowel Go and C. Kumar N. Patel, "Multiwatt Long Wavelength Quantum Cascade Lasers Based on High Strain Composition with 70% Injection Efficiency", *Optics Express* **20,** 24272-24279 (2012).

[9] Y. Bai, N. Bandyopadhyay, S. Tsao, S. Slivken, and M. Razeghi, "Room Temperature Quantum Cascade Lasers with 27% Wall Plug Efficiency", *Appl. Phys. Lett.* **98**, 181102 (2011).

[10] A. Lyakh, M. Suttinger, R. Go, P. Figueiredo, and A. Todi, "5.6 µm Quantum Cascade Lasers Based on a Two-Material Active Region Composition with a Room Temperature Wall-Plug Efficiency Exceeding 28%", *Appl. Phys. Lett.* 109, 121109 (2016).

[11] M. Suttinger, R. Go, P. Figueiredo, A. Todi, Hong Hsu, and A. Lyakh, E. Tsvid and C. Kumar N. Patel Narrow Ridge Buried Heterostructure Continuous Wave Quantum Cascade Lasers with Reduced Number of Stages", *Proc. SPIE,* Paper 10194-96 (to be published).

[12] Arkadiy Lyakh and C. Kumar N. Patel "Quantum Cascade Lasers with Reduced Number of Active Region Stages", (U. S. Patent Application).

[13] Arkadiy Lyakh, Rodolfo Barron-Jimenez, Ilya Dunayevskiy, Rowel Go and C. Kumar N. Patel, "External Cavity Quantum Cascade Lasers with Ultra Rapid Acousto-optic Tuning", *Appl. Phys. Lett.* **106**, 141101 (2015).

[14] D. J. Taylor, S. E. Harris, S. T. K. Nieh and T. W. Hänsch, "Electronic Tuning of a Dye Laser Using the Acousto-Optic Filter", *Appl. Phys. Lett.* **19,** 269-271 (1971).

[15] G. A. Coquin and K. W. Cheung, "Electronically Tunable External Cavity Semiconductor Laser", *Electron. Lett.* **24,** 599-600 (1988).

[16] A. Lyakh, R. Barron-Jimenez, I. Dunayevskiy, R. Go, G. Tsvid, and C. Kumar N. Patel, "Continuous Wave Operation of Quantum Cascade Lasers with Frequency-Shifted Feedback, *AIP Advances* **6**, 015312 (2016).

[17] C. Kumar N. Patel, Rodolfo Barron-Jimenez, Ilya Dunayevskiy, Gene Tsvid, and Arkadiy Lyakh, "Two Wavelength Operation of an Acousto-Optically Tuned Quantum Cascade Laser and Direct Measurements of Quantum Cascade Laser Level Lifetimes", *Appl. Phys. Lett.* **110**, 031104 (2017).

[18] Gerald Coquin and Kwok-Wai Cheung "Single- and Multiple-Wavelength Operation of Acousto-optically Tuned Semiconductor Lasers at 1.3 µm", *IEEE JQE* **25**, 1575-1579 (1989).